

Shape of pendant droplets under a tilted surface

Joël De Coninck and Juan Carlos Fernández-Toledano
Laboratoire de Physique des Surfaces et Interfaces
Université de Mons, 20 Place du Parc, 7000 Mons, Belgium

François Dunlop, Thierry Huillet, and Alvin Sodji
Laboratoire de Physique Théorique et Modélisation, CNRS-UMR 8089
Université de Cergy-Pontoise, 95302 Cergy-Pontoise, France

For a pendant drop whose contact line is a circle of radius r_0 , we derive the relation $mg \sin \alpha = \frac{\pi}{2} \gamma r_0 (\cos \theta^{\min} - \cos \theta^{\max})$ at first order in the Bond number, where θ^{\min} and θ^{\max} are the contact angles at the back (uphill) and at the front (downhill), m is the mass of the drop and γ the surface tension of the liquid. The Bond (or Eötvös) number is taken as $Bo = mg/(2r_0\gamma)$. The tilt angle α may increase from $\alpha = 0$ (sessile drop) to $\alpha = \pi/2$ (drop pinned on vertical wall) to $\alpha = \pi$ (drop pendant from ceiling). The focus will be on pendant drops with $\alpha = \pi/2$ and $\alpha = 3\pi/4$. The drop profile is computed exactly, in the same approximation. Results are compared with *surface evolver* simulations, showing good agreement up to about $Bo = 1.2$, corresponding for example to hemispherical water droplets of volume up to about $50 \mu\text{L}$. An explicit formula for each contact angle θ^{\min} and θ^{\max} is also given and compared with the almost exact *surface evolver* values.

PACS numbers: 47.55.D-, 68.03.Cd, 68.08.Bc, 47.10.A-, 47.11.Fg

I. INTRODUCTION

The study of static contact angles and shapes of both sessile and pendant drops on a substrate has been an important issue in engineering sciences, including: drop condensation [1], biomedical (or biological) microelectromechanical systems, drug delivery, to cite only a few. Contact angles give information about wettability and surface energy. The three-phase contact angles of a liquid condensed on a substrate is in direct relation with interfacial and body forces acting on sessile or pendant drops. In spite of abundance of data on contact angles for sessile drops, there is a gap in the knowledge of contact angles of pendant drops on inclined surfaces. Pendant drops appear to be difficult to deal with in experiments.

Drops on vertical window panes is an important issue to design self-cleaning surfaces. Also the problem of a bubble pinned on top of a plate is amenable to the one of a pendant drop, pinned underneath [2, 3]. Another application is pendant drop tensiometry where a droplet is suspended from a needle [4]. Cheng et al. [5] performed experiments to measure contact angles of pendant axisymmetric glycerin and water drops. When the surface on which the pendant drop is deposited is inclined with respect to the horizontal, the angle downhill is greater than the angle uphill. These angles are a function of plate inclination. Overall, the drop is deformed and becomes non-axisymmetric. Several authors [6–8] have discussed the effect of plate inclination on the contact angles of sessile drops. A sessile drop may be understood as one in equilibrium resting on a flat surface while a pendant drop is one which hangs from a ceiling or a wall. Though the equations describing the shape of both drops are similar, the body forces have opposing effects tending in the former case to flatten the drop and in the latter one to elongate its shape, possibly resulting in a neck region.

The effect of plate inclination breaks the axisymmetry of the problem.

The effect of surface chemistry of solid-liquid combinations on contact angles clearly is an active subject of research. Factors such as surface energy, wettability and substrate vibration or oscillation [9] also affect contact angles. Temperature is also an independent control variable.

Understanding the shape of a drop pinned on an incline has a long history in Physics, starting with [10, 11]. An empirical relation between slope angle and contact angles was given by Furmidge [12], and further studied by many authors, see [8, 13] and references therein. More recently the case of pendant drops has attracted much interest [14–16], [17] and references therein.

In the present work, we limit ourselves to the analysis of the effect of inclination and drop volume on contact angles for pinned pendant drops, which are subject to the Laplace-Young equation. This is a non-linear partial differential equation of second order, for a two-dimensional surface. More can be done mathematically and numerically in the case of cylindrical symmetry, $\alpha = 0$ or π with circular contact line [4, 18, 19]. There the Laplace-Young equation takes the form of an ordinary differential equation. In the present work we focus on the asymmetrical case, $\alpha \notin \{0, \pi\}$, requiring partial differential equations techniques, illustrated with $\alpha = \pi/2$ and $\alpha = 3\pi/4$. We perform the calculations for gravity but the technique can easily be adapted to other distorting forces, associated with electric or magnetic fields.

In [8] we derived a linear response solution to the Laplace-Young equation for a drop sitting on an incline, using cylindrical coordinates. In the present paper we use spherical coordinates, covering a wider range of contact angles, and including the pendant drop problem.

In Section II we give the setting in spherical coordi-

nates and introduce a linear response ansatz to solve the Laplace-Young equation at first order in the Bond number. In Section III we show that the ansatz implies the Furmidge relation described in the abstract and we test its validity against *surface evolver* simulations. A comparison is given between the pendant drop ($\alpha = 135$ degrees) and the sessile drop ($\alpha = 45$ degrees). In Section IV we derive exact solutions for drop profiles at first order in the Bond number and compare them with *surface evolver* simulations. In Section V we compute separately, in the same approximation, each contact angle and compare the predictions with *surface evolver* results. In Section VI we comment on the technical aspects of the approximate numerical solution with *surface evolver*. In Section VII we summarize the results and give a perspective.

II. LAPLACE-YOUNG EQUATION IN SPHERICAL COORDINATES

The Laplace-Young equation equates the Laplace pressure to the hydrostatic pressure:

$$p_{\text{liq}} = p_{\text{atm}} - 2\gamma H = p_0 + \rho \mathbf{g} \cdot \mathbf{r}, \quad H = \frac{1}{2} \left(\frac{1}{R_1} + \frac{1}{R_2} \right) \quad (1)$$

where p_0 is the pressure at the origin and H is the mean curvature defined with the outer normal pointing from the liquid into the atmosphere: each principal radius of curvature is positive when the corresponding center of curvature is on the side of the outer normal and negative otherwise.

The Cartesian frame of reference has z -axis perpendicular to the substrate, pointing from the substrate into the liquid, x -axis along the slope downwards, and y -axis horizontal, so that the corresponding unit vectors satisfy $\mathbf{e}_x \wedge \mathbf{e}_y = \mathbf{e}_z$. The slope angle $\alpha \in [0, \pi]$ corresponds to a rotation of angle α of the system and frame of reference around the y -axis, so that the gravity vector $\mathbf{g} = (g \sin \alpha, 0, -g \cos \alpha)$. Thus $\alpha = 0$ is a sessile drop on a horizontal substrate, $\alpha = \pi/2$ is a drop pinned on a vertical wall, $\alpha = \pi$ is a drop pendant from the ceiling. We use spherical polar coordinates with origin at the center of the spherical cap at zero gravity, $\theta \in [0, \theta_0]$ measured from the z -axis and azimuth $\varphi \in [-\pi, \pi]$ measured from the x -axis. Then (1) reads

$$p_{\text{atm}} - 2\gamma H = p_0 - \rho g r \cos \alpha \cos \theta + \rho g r \sin \alpha \sin \theta \cos \varphi \quad (2)$$

a partial differential equation for the drop profile $r(\theta, \varphi)$. At zero gravity we have a spherical cap of volume V , radius R and contact angle θ_0 such that $r_0 = R \sin \theta_0$ and

$$\begin{aligned} V &= \pi R^3 \left(\frac{2}{3} - \cos \theta_0 + \frac{1}{3} \cos^3 \theta_0 \right) \\ &= \frac{\pi R^3}{3} (1 - \cos \theta_0)^2 (2 + \cos \theta_0) \end{aligned} \quad (3)$$

The boundary condition for (2) is $r(\theta_0, \varphi) = R \forall \varphi$, and volume conservation implies

$$\int_0^{\theta_0} \sin \theta d\theta \int_{-\pi}^{\pi} d\varphi \int_0^{r(\theta, \varphi)} r^2 dr = V \quad (4)$$

In order to convert (2) to a dimensionless equation and reduce the number of parameters, let

$$r = R\tilde{r}, \quad H = R^{-1}\tilde{H}, \quad p = \gamma R^{-1}\tilde{p} \quad (5)$$

Then (2) takes the form of the adimensional Laplace-Young equation

$$\tilde{p}_{\text{atm}} - 2\tilde{H} = \tilde{p}_0 - B\tilde{r} \cos \alpha \cos \theta + B\tilde{r} \sin \alpha \sin \theta \cos \varphi \quad (6)$$

where B is the Bond number associated to the length R ,

$$B = \frac{\rho g R^2}{\gamma} \quad (7)$$

When comparing with *surface evolver* simulations, we will use

$$Bo = \frac{mg}{w\gamma} = \frac{mg}{2r_0\gamma} = \frac{B\pi(1 - \cos \theta_0)^2(2 + \cos \theta_0)}{6 \sin \theta_0} \quad (8)$$

where w is the width of the drop basis, here equal to $2r_0$. We have three independent parameters: α , θ_0 , and B or Bo . The pressure difference $\tilde{p}_0 - \tilde{p}_{\text{atm}}$ will be determined from volume conservation.

At small B , an approximate solution to (6) may be obtained by a linear response argument: the deformation from the spherical cap is caused by the two terms linear in B . As functions of the azimuth φ these terms generate a two-dimensional vector space, linear combinations $a + b \cos \varphi$ with a, b functions of θ . The linear response ansatz consists in looking for a solution to (6) in this vector space, at first order in B :

$$\tilde{r}(\theta, \varphi) = 1 + B r_{01}(\theta) \cos \alpha + B r_{11}(\theta) \sin \alpha \cos \varphi + O(B^2) \quad (9)$$

where $r_{01}(\theta)$ and $r_{11}(\theta)$ are arbitrary functions of θ , subject to the boundary conditions, and also subject to volume conservation at first order in B .

In [8], linear response was used in cylindrical coordinates, with

$$z(r, \varphi) = z_{00}(r) + B z_{01}(r) \cos \alpha + B z_{11}(r) \sin \alpha \cos \varphi + O(B^2) \quad (10)$$

where $z_{00}(r)$ is the spherical cap profile. The change of variables between spherical and cylindrical coordinates is non-linear. Therefore the drop profiles derived from linear response in either coordinates will differ by an $O(B^2)$.

Also the drop volume is a linear functional of $z(r, \varphi)$ in cylindrical coordinates, but a non-linear functional of $r(\theta, \varphi)$ in spherical coordinates. This will also contribute a difference $O(B^2)$ when imposing volume conservation at first order in B .

III. THE FURMIDGE RELATION

The ansatz (9) already implies the Furmidge relation [12] as stated in the abstract, following the argument in [8]. Indeed let $\theta_\alpha(\varphi)$ be the contact angle at azimuth φ . Then $\cos\theta_\alpha(\varphi)$ may be computed from (9), using $r_{01}(\theta)$ and $r_{11}(\theta)$ and their derivatives at $\theta = \theta_0$. The result as function of φ , at first order in B , will again be in the linear span of constants and $\cos\varphi$. The values at $\varphi = 0$ and $\varphi = \pi$ determine the linear combination:

$$\cos\theta_\alpha(\varphi) = \frac{\cos\theta_\alpha^{\min} + \cos\theta_\alpha^{\max}}{2} - \cos\varphi \frac{\cos\theta_\alpha^{\min} - \cos\theta_\alpha^{\max}}{2} \quad (11)$$

where $\theta_\alpha^{\min} = \theta_\alpha(\pi)$ and $\theta_\alpha^{\max} = \theta_\alpha(0)$ are the contact angles at the back (uphill) and at the front (downhill). This allows to compute the capillary force upon the drop, component parallel to the substrate plane, a force which lies in the negative direction of the x -axis:

$$\begin{aligned} F_\gamma &= \int_{-\pi}^{\pi} r_0 d\varphi \cos\varphi \cos\theta_\alpha(\varphi) \\ &= -\frac{\pi}{2} \gamma r_0 (\cos\theta_\alpha^{\min} - \cos\theta_\alpha^{\max}) + O(B^2) \end{aligned} \quad (12)$$

Balance with gravity implies the desired Furmidge relation,

$$mg \sin\alpha = \frac{\pi}{2} \gamma r_0 (\cos\theta_\alpha^{\min} - \cos\theta_\alpha^{\max}) + O(B^2) \quad (13)$$

We define the Furmidge ratio as

$$Fu = \frac{\pi \gamma r_0 (\cos\theta_\alpha^{\min} - \cos\theta_\alpha^{\max})}{2 mg \sin\alpha} \quad (14)$$

obeying $Fu = 1 + O(B)$.

Therefore (14) with $Fu = 1$ gives a prediction at first order in B of $\cos\theta_\alpha^{\min} - \cos\theta_\alpha^{\max}$. We have simulated water droplets with *surface evolver*, and measured θ_α^{\min} and θ_α^{\max} , whence Fu , plotted in Fig. 1.

The drop will de-pin when θ_α^{\max} will increase up to the advancing angle $\theta^{\text{advancing}}$ or when θ_α^{\min} will decrease down to the receding angle θ^{receding} . Therefore the larger Fu the closer to de-pinning. $Fu > 1$ means that the correction to linear response brings the drop closer to the depinning instability. This is also clear on the drop profiles, as in Fig. 2.

IV. SOLUTION AT FIRST ORDER IN B .

The mean curvature \tilde{H} is given by

$$-2\tilde{H} = \nabla \cdot \mathbf{n} \quad (15)$$

The normal to a surface of equation $f(r, \theta, \varphi) = 0$ is

$$\mathbf{n} = \nabla f / \|\nabla f\| \quad (16)$$

Hence, using the gradient in spherical coordinates, and now denoting simply r the adimensional radial coordinate,

$$\begin{aligned} \mathbf{n} &= \nabla \left[r - 1 - B r_{01}(\theta) \cos\alpha - B r_{11}(\theta) \sin\alpha \cos\varphi \right] \\ &\quad + O(B^2) \\ &= \mathbf{u}_r - B \left(\frac{r'_{01}(\theta)}{r} \cos\alpha + \frac{r'_{11}(\theta)}{r} \sin\alpha \cos\varphi \right) \mathbf{u}_\theta \\ &\quad + B \frac{r_{11}(\theta)}{r \sin\theta} \sin\alpha \sin\varphi \mathbf{u}_\varphi + O(B^2) \end{aligned} \quad (17)$$

where $\|\nabla f\| = 1 + O(B^2)$ has been used. Then

$$\begin{aligned} -2\tilde{H} &= \nabla \cdot \mathbf{n} \\ &= \frac{2}{r} - B \left[\frac{r''_{01}(\theta)}{r^2} \cos\alpha + \frac{r''_{11}(\theta)}{r^2} \sin\alpha \cos\varphi \right. \\ &\quad \left. + \frac{r'_{01}(\theta) \cot\theta}{r^2} \cos\alpha \right. \\ &\quad \left. + \frac{r'_{11}(\theta) \cot\theta}{r^2} \sin\alpha \cos\varphi - \frac{r_{11}(\theta)}{r^2 \sin^2\theta} \sin\alpha \cos\varphi \right] + O(B^2) \\ &= -2\tilde{H}_0 - 2B\tilde{H}_{01} \cos\alpha - 2B\tilde{H}_{11} \sin\alpha \cos\varphi + O(B^2) \end{aligned} \quad (18)$$

with, at $r = \tilde{r}(\theta, \varphi)$ as (9),

$$\begin{aligned} -2\tilde{H}_0 &= 2 \\ -2\tilde{H}_{01} &= -2r_{01}(\theta) - r''_{01}(\theta) - r'_{01}(\theta) \cot\theta \\ -2\tilde{H}_{11} &= -2r_{11}(\theta) - r''_{11}(\theta) - r'_{11}(\theta) \cot\theta + \frac{r_{11}(\theta)}{\sin^2\theta} \end{aligned} \quad (19)$$

Similarly

$$\tilde{p}_0 = \tilde{p}_{00} + B\tilde{p}_1 \cos\alpha + O(B^2) \quad (20)$$

Order 0 in B for (6) is the Laplace equation

$$\tilde{p}_{\text{atm}} + 2 = \tilde{p}_{00} \quad (21)$$

Order one in B for (6) has terms independent of φ and terms linear in $\cos\varphi$, hence two ordinary differential equations

$$\begin{aligned} -2\tilde{H}_{01} &= \tilde{p}_1 - \cos\theta \\ -2\tilde{H}_{11} &= \sin\theta \end{aligned}$$

or

$$\begin{aligned} r''_{01}(\theta) + r'_{01}(\theta) \cot\theta + 2r_{01}(\theta) &= \cos\theta - \tilde{p}_1 \\ r''_{11}(\theta) + r'_{11}(\theta) \cot\theta + r_{11}(\theta)(1 - \cot^2\theta) &= -\sin\theta \end{aligned} \quad (22)$$

for $\theta \in [0, \theta_0]$ with boundary conditions

$$\begin{aligned} r'_{01}(0) = 0, r_{01}(\theta_0) = 0 \\ r'_{11}(0) = 0, r_{11}(\theta_0) = 0 \end{aligned} \quad (23)$$

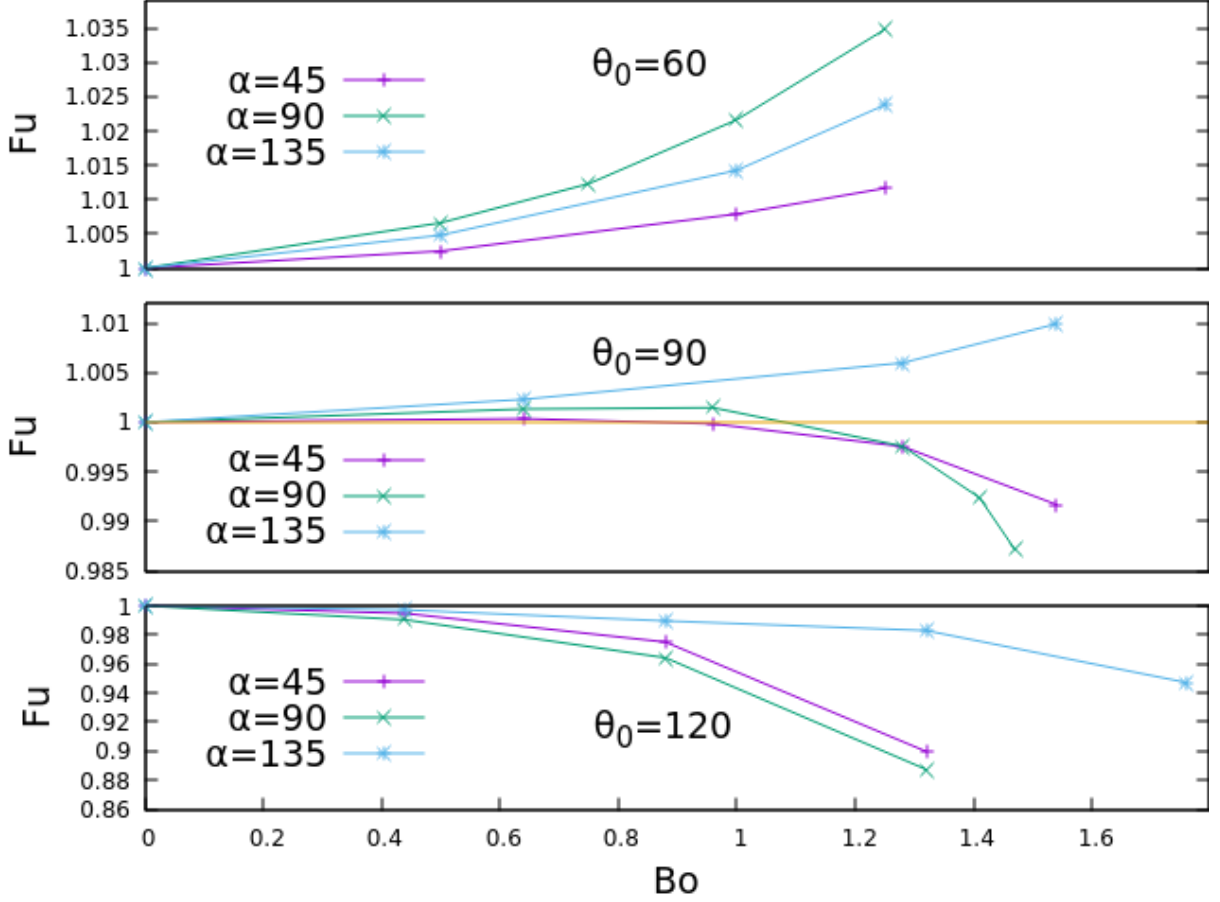


FIG. 1. Furmidge ratio Fu (14) for $\theta_0 = 60, 90, 120$ degrees and $\alpha = 45, 90, 135$ degrees versus Bond number Bo (8).

Hence two parameters: $\theta_0 \in [0, \pi]$ and $\tilde{p}_1 \in \mathbb{R}$. The ordinary differential equations (22) with boundary conditions (23) are solved exactly with *Mathematica*:

$$\begin{aligned} r_{01}(\theta) &= \cos \theta \left[C_{01} - \frac{1}{3} \log(1 + \cos \theta) \right] + \frac{2 - 3\tilde{p}_1}{6} \\ r_{11}(\theta) &= \sin \theta \left[C_{11} + \frac{1}{3} \log(1 + \cos \theta) \right] + \frac{\cos \theta - \cos^2 \theta}{3 \sin \theta} \end{aligned} \quad (24)$$

with C_{11} from $r_{11}(\theta_0) = 0$,

$$C_{11} = -\frac{\cos \theta_0}{3(1 + \cos \theta_0)} - \frac{1}{3} \log(1 + \cos \theta_0) \quad (25)$$

and C_{01}, \tilde{p}_1 from $r_{01}(\theta_0) = 0$ and volume conservation at first order in B ,

$$\int_0^{\theta_0} r_{01}(\theta) \sin \theta d\theta = 0 \quad (26)$$

entailing

$$C_{01} = \frac{1}{6} + \frac{1}{3} \log(1 + \cos \theta_0); \quad \tilde{p}_1 = \frac{2 + \cos \theta_0}{3} \quad (27)$$

Then

$$\begin{aligned} r_{01}(\theta) &= \frac{\cos \theta - \cos \theta_0}{6} + \frac{\cos \theta}{3} \log \frac{1 + \cos \theta}{1 + \cos \theta_0} \\ r_{11}(\theta) &= \frac{\sin \theta}{3} \left[\frac{\cos \theta}{1 + \cos \theta} - \frac{\cos \theta_0}{1 + \cos \theta_0} + \log \frac{1 + \cos \theta}{1 + \cos \theta_0} \right] \end{aligned} \quad (28)$$

$$(29)$$

We can now easily plot the linear response drop profiles by inserting (28)(29) into (9) without $O(B^2)$, and compare with *surface evolver* profiles: Fig. 2, computed for water droplets, $\rho = 997 \text{ kg/m}^3$, $g = 9.8 \text{ m/s}^2$, $\gamma = 0.073 \text{ N/m}$. The values of Bo were chosen so that there is a significant difference between the two. At half these Bond numbers the profiles almost coincide. At twice these Bond numbers, the Laplace-Young equation under the given conditions does not have a well defined solution.

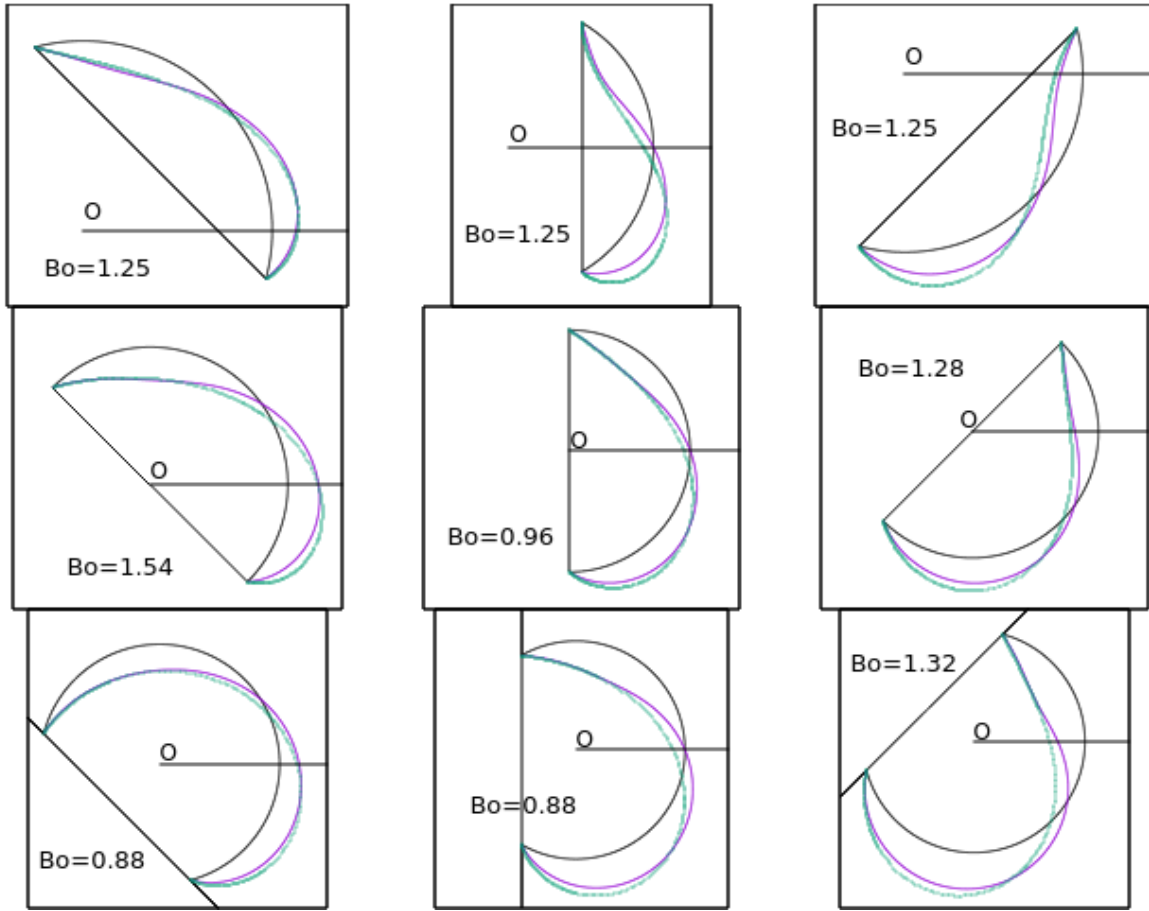


FIG. 2. Droplet profiles for $\theta_0 = 60, 90, 120$ degrees (from top to bottom) and $\alpha = 45, 90, 135$ degrees (from left to right), Bond numbers as shown. Green-blue points: surface evolver. Purple lines: linear response from (9)(27)(28). Black: spherical cap of same volume, centred at O , with contact angle θ_0 .

V. CONTACT ANGLES

The contact angle $\theta = \theta(\varphi)$ is given by

$$\cos \theta = \mathbf{u}_\rho \cdot \left. \frac{\partial \tilde{\mathbf{r}} / \partial \theta}{|\partial \tilde{\mathbf{r}} / \partial \theta|} \right|_{\theta=\theta_0} \quad (30)$$

where $\mathbf{u}_\rho = \cos \theta \mathbf{u}_\theta + \sin \theta \mathbf{u}_r$ is the radial unit vector of plane polar coordinates associated with the contact line circle. We shall compute contact angles exactly for the linear response profile, namely (9) without the $O(B^2)$ correction:

$$\tilde{\mathbf{r}} = \tilde{r}(\theta, \varphi) \mathbf{u}_r \quad (31)$$

$$\left. \frac{\partial \tilde{\mathbf{r}}}{\partial \theta} \right|_{\theta=\theta_0} = \mathbf{u}_\theta + B(r'_{01}(\theta_0) \cos \alpha + r'_{11}(\theta_0) \sin \alpha \cos \varphi) \mathbf{u}_r \quad (32)$$

$$\cos \theta = \frac{\cos \theta_0 + B(r'_{01}(\theta_0) \cos \alpha + r'_{11}(\theta_0) \sin \alpha \cos \varphi) \sin \theta_0}{(1 + B^2(r'_{01}(\theta_0) \cos \alpha + r'_{11}(\theta_0) \sin \alpha \cos \varphi)^2)^{1/2}} \quad (33)$$

with, from (28)(29),

$$r'_{01}(\theta_0) = -\sin \theta_0 / 6 + \sin \theta_0 \cos \theta_0 / (3(1 + \cos \theta_0))$$

$$r'_{11}(\theta_0) = \cos \theta_0 / 3 - 2 / (3(1 + \cos \theta_0))$$

Then $\cos \theta^{\max}$ is given by (33) with $\varphi = 0$ and $\cos \theta^{\min}$ with $\varphi = \pi$. The corresponding contact angles θ^{\min} and θ^{\max} are plotted for $\alpha = 45$ degrees on Fig. 3, for $\alpha = 90$ degrees on Fig. 4, for $\alpha = 135$ degrees on Fig. 5, together with the almost exact *surface evolver* values. Increasing Bo at constant θ_0 corresponds to scaling up all length scales, drop and its basis alike.

The dimensionless variables Bo (ratio of gravity over capillarity) and θ_0 (contact angle at zero gravity) may be related to V and r_0 through

$$Bo = \frac{\rho g V}{2\gamma r_0} \quad (34)$$

$$\frac{(1 - \cos \theta_0)^2 (2 + \cos \theta_0)}{\sin^3 \theta_0} = \frac{3V}{\pi r_0^3}$$

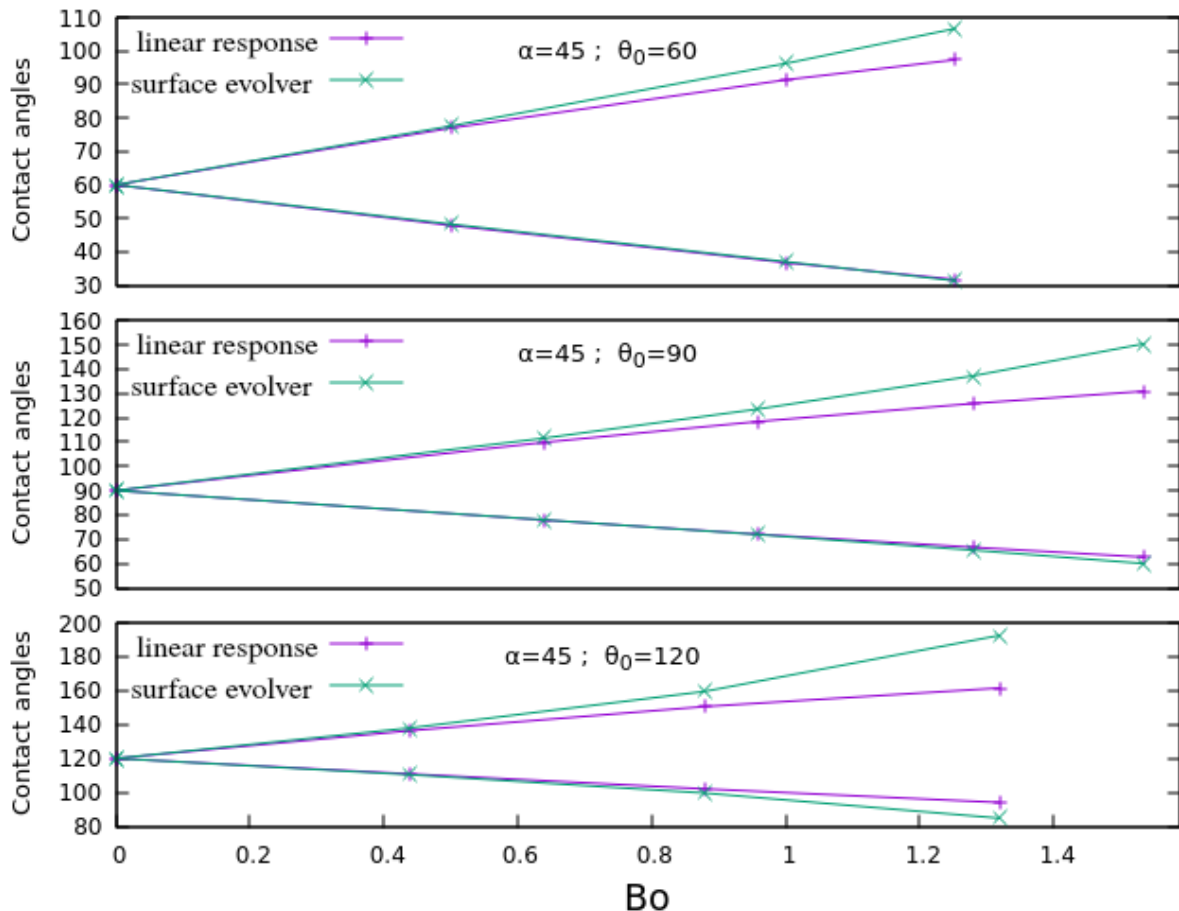


FIG. 3. Contact angles θ^{\min} and θ^{\max} as function of Bo for $\alpha = 45$ degrees and $\theta_0 = 60, 90, 120$ degrees. Linear response from (33).

or

$$\begin{aligned}
 r_0^2 &= \frac{6\gamma}{\pi\rho g} \frac{Bo \sin^3 \theta_0}{(1 - \cos \theta_0)^2 (2 + \cos \theta_0)} \\
 V &= \frac{2\gamma r_0}{\rho g} Bo
 \end{aligned}
 \tag{35}$$

VI. SURFACE EVOLVER

The approximate numerical solutions of the Laplace-Young equation under the given conditions were obtained with the finite elements software *Surface evolver*. A fine mesh implies slow convergence in time (number of iterations) due in particular to the vicinity of zero modes (capillary waves), weakly damped by gravity. We used linear elements, for which convergence in the number of elements or vertices goes like the inverse of that number, again a slow convergence. The asymptotic values of the Fumridge coefficient Fu were obtained by a least squares fit to $a + b/(\text{number of vertices})$, with up to 82000 ver-

tices. Altogether each point in Fig. 1, or each drop profile in Fig. 2 required about 15h of CPU.

VII. CONCLUSION

We have studied pendant drops pinned under an incline of tilt angle $\alpha \in [\pi/2, \pi)$, with a circular contact line and contact angle $\theta_\alpha(\varphi)$ at azimuth φ obeying

$$0 \leq \theta^{\text{receding}} \leq \theta_\alpha^{\min} \leq \theta_\alpha(\varphi) \leq \theta_\alpha^{\max} \leq \theta^{\text{advancing}} \leq \pi,$$

thus for a very large range of contact angles. We have illustrated the results with $\alpha = \pi/2$ and $\alpha = 3\pi/4$.

In such situations, the axisymmetry of the problem is broken and the shape of the drops can only be handled by the non-linear Laplace-Young partial differential equation. We developed a linear response ansatz leading to an exact integrable solution of the Laplace-Young equation at first order in a Bond number. The use of spherical coordinates was shown particularly relevant for the pendant drop problem. Comparison of the obtained approximate drop profiles with *surface evolver* simulations

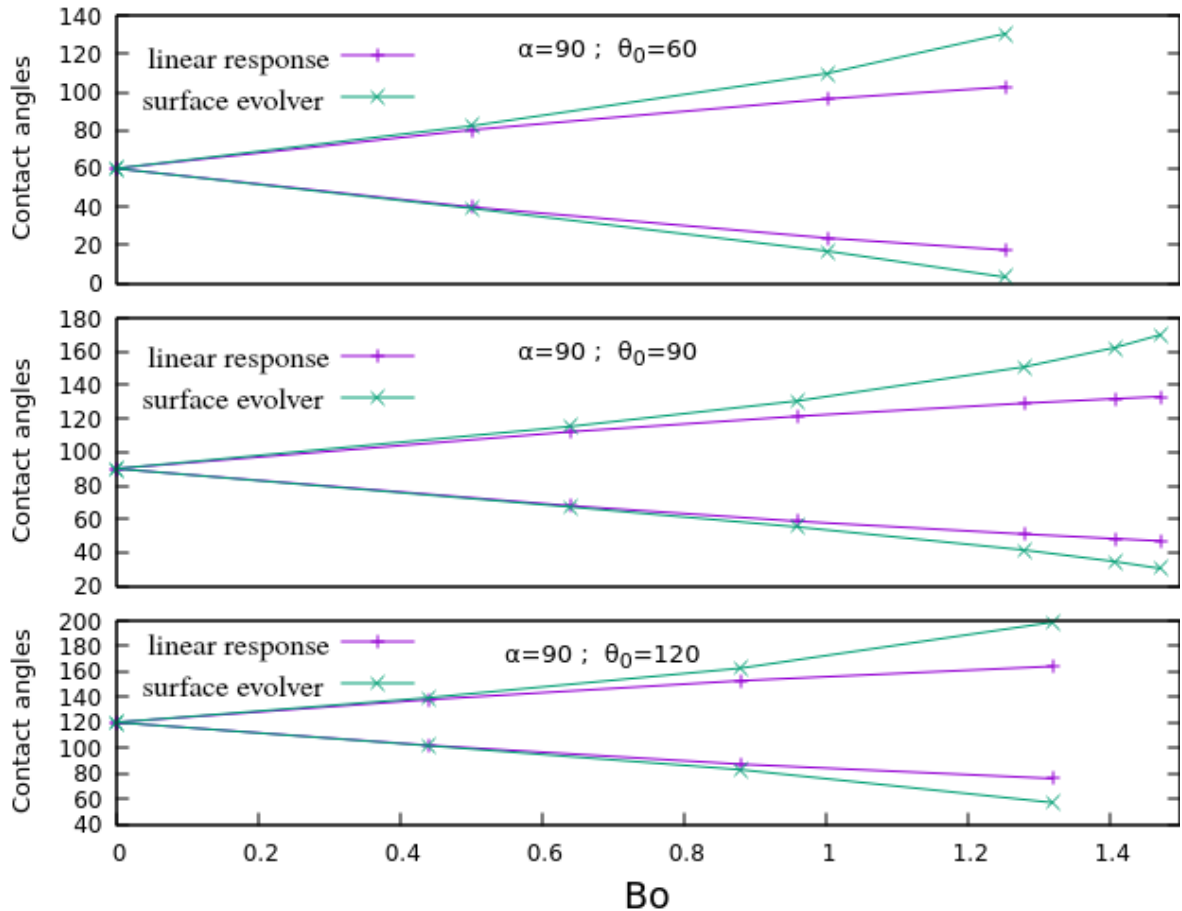


FIG. 4. Contact angles θ^{\min} and θ^{\max} as function of Bo for $\alpha = 90$ degrees and $\theta_0 = 60, 90, 120$ degrees. Linear response from (33).

showed good agreement for Bond numbers up to about $Bo = 1.2$, corresponding for example to hemispherical water droplets with volume up to about 50 mm^3 . The linear response ansatz has also been shown to imply the (small Bond number) Furmidge-like relation described in the abstract, translating a balance between capillary force and gravity; the validity of this relation was successfully tested against *surface evolver* simulations. It would be interesting to better identify the upper value of the Bond number at which this relation starts failing. We also derived a small Bond number expression for the contact angles, showing good agreement with the simulations.

Sessile drops are less sensitive to gravity than pendant drops. For comparison with the earlier work [8] therefore, we included the study of a sessile drop pinned on an incline of tilt angle $\alpha = \pi/4$.

ACKNOWLEDGMENTS

The authors thank the European Space Agency (ESA) and the Belgian Federal Science Policy Office (BELSPO) for their support in the framework of the PRODEX Programme. This research was also partially funded by the Inter-University Attraction Poles Programme (IAP 7/38 MicroMAST) of the Belgian Science Policy Office, FNRS and Région Wallonne.

-
- [1] B. Sikarwar, N. Battoo, S. Khandekar, and K. Muralidhar, *ASME Journal of Heat Transfer* **133**(2), 021501 (2011).
 [2] Y. Nama, E. Aktinol, V. K. Dhir, and Y. S. Ju, *International Journal of Heat and Mass Transfer* **54**, 1572

- (2011).
 [3] P. Aussillous and D. Quéré, *Europhys. Lett.* **59**, 370 (2002).
 [4] J. D. Berry, M. J. Neeson, R. R. Dagastine, D. Y. Chan, and R. F. Tabor, *J. Colloid Interface Sci.* **454**, 226 (2015).

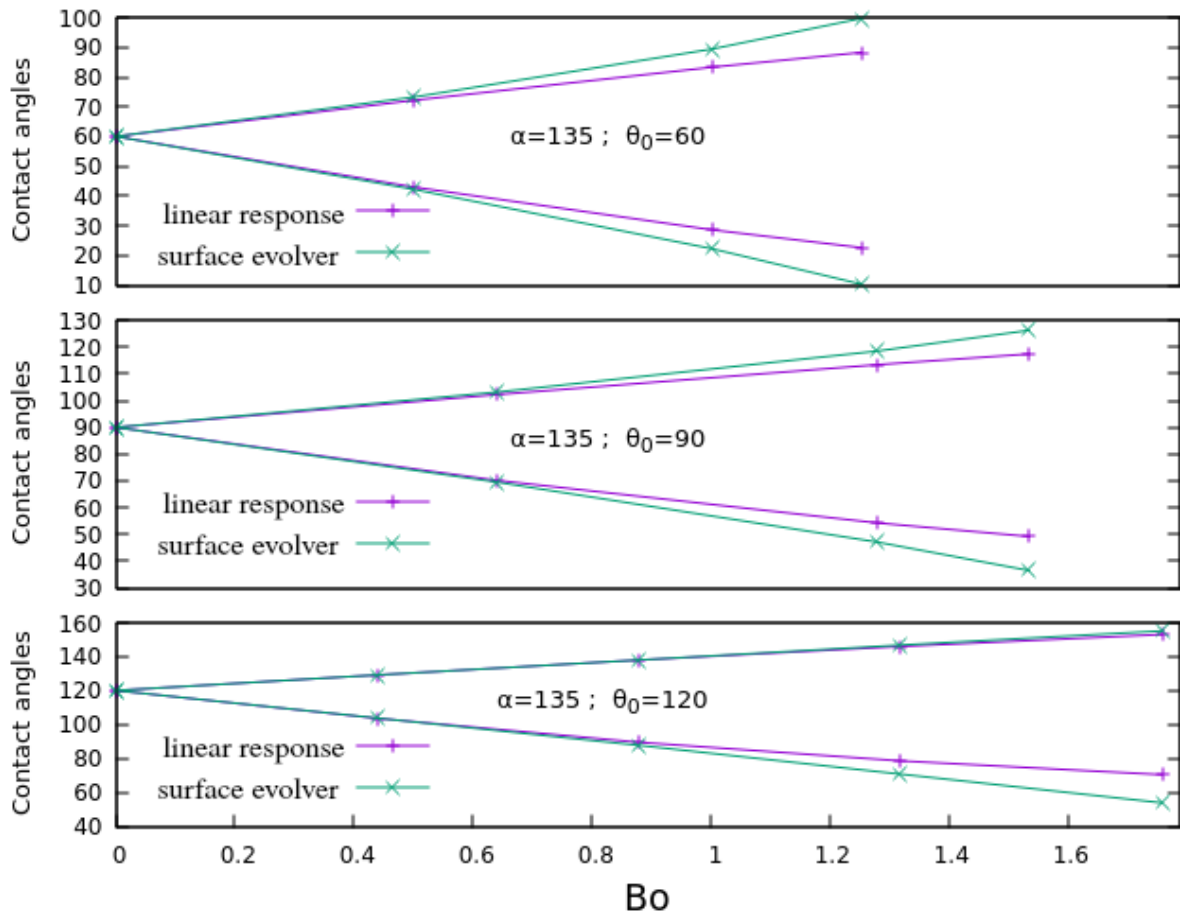


FIG. 5. Contact angles θ^{\min} and θ^{\max} as function of Bo for $\alpha = 135$ degrees and $\theta_0 = 60, 90, 120$ degrees. Linear response from (33).

- [5] P. Cheng, D. Li, L. Boruvka, Y. Rotenberg, and A. Neumann, *Colloids and Surfaces* **43**, 151 (1990).
- [6] R. A. Brown, F. M. Orr, Jr., and L. E. Scriven, *J. Colloid Interface Sci.* **73**, 76 (1980).
- [7] A. ElSherbini and A. Jacobi, *J. Colloid Interface Sci.* **273**, 556 (2004).
- [8] J. De Coninck, F. Dunlop, and T. Huillet, *Phys. Rev. E* **95**, 052805 (2017).
- [9] L. De Maio and F. Dunlop, *Journal of Applied Fluid Mechanics* **11(6)**, 1471 (2018).
- [10] G. Macdougall and C. Ockrent, *Proc. R. Soc. London Ser. A* **180**, 151 (1942).
- [11] Y. I. Frenkel, *Zh. Eksp. Teor. Fiz.* **18**, 659 (1948 (Translated by V. Berejnov: <http://xxx.lanl.gov/abs/physics/0503051>)).
- [12] C. G. L. Furnidge, *J. Colloid Science* **17**, 309 (1962).
- [13] A. ElSherbini and A. Jacobi, *J. Colloid Interface Sci.* **299**, 841 (2006).
- [14] F. Milinazzo and M. Shinbrot, *J. Colloid. Interface Sci.* **121**, 254 (1988).
- [15] G. Bhutani, S. Khandekar, and K. V. Muralidhar, *Proceedings of the Thirty Ninth National Conference on Fluid Mechanics and Fluid Power, Gujarat, India* (2012).
- [16] R. de la Madrid, T. Whitehead, and G. Irwin, *Am. J. Phys.* **83**, 531 (2015).
- [17] R. de la Madrid, F. Garza, J. Kirk, H. Luong, L. Snowden, J. Taylor, and B. Vizena, *Langmuir* **35(7)**, 2871 (2019).
- [18] S. B. G. O'Brien, *J. Fluid Mech.* **233**, 519 (1991).
- [19] A. H. Fatollahi and M. Hajirahimi, *arXiv:1304.6366 [cond-mat.soft]* (2013).